

Electron-electron interaction effects on the photophysics of metallic single-walled carbon nanotubes

Zhendong Wang, Demetra Psiachos, Roberto F. Badilla, and Sumit Mazumdar

Department of Physics, University of Arizona Tucson, AZ 85721

(Dated: November 11, 2018)

Abstract

Single-walled carbon nanotubes are strongly correlated systems with large Coulomb repulsion between two electrons occupying the same p_z orbital. Within a molecular Hamiltonian appropriate for correlated π -electron systems, we show that optical excitations polarized parallel to the nanotube axes in the so-called metallic single-walled carbon nanotubes are to excitons. Our calculated absolute exciton energies in twelve different metallic single-walled carbon nanotubes, with diameters in the range 0.8 - 1.4 nm, are in nearly quantitative agreement with experimental results. We have also calculated the absorption spectrum for the (21,21) single-walled carbon nanotube in the E_{22} region. Our calculated spectrum gives an excellent fit to the experimental absorption spectrum. In all cases our calculated exciton binding energies are only slightly smaller than those of semiconducting nanotubes with comparable diameters, in contradiction to results obtained within the *ab initio* approach, which predicts much smaller binding energies. We ascribe this difference to the difficulty of determining the behavior of systems with strong on-site Coulomb interactions within theories based on the density functional approach. As in the semiconducting nanotubes we predict in the metallic nanotubes a two-photon exciton above the lowest longitudinally polarized exciton that can be detected by ultrafast pump-probe spectroscopy. We also predict a subgap absorption polarized perpendicular to the nanotube axes below the lowest longitudinal exciton, blueshifted from the exact midgap by electron-electron interactions.

PACS numbers: 73.22.-f, 78.67.Ch, 71.35.-y

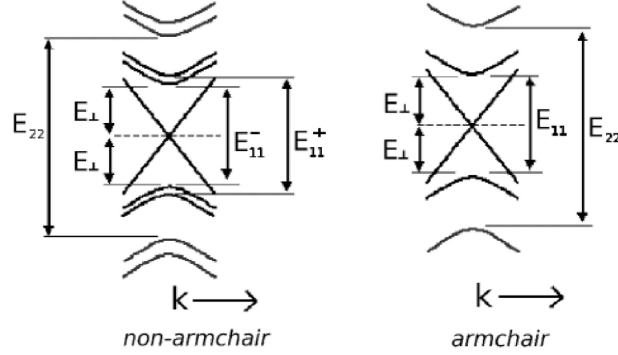


FIG. 1: (a) Schematics of the tight-binding band structures of M-SWCNTs and longitudinal and transverse optical transitions within one-electron theory. Splittings due to the trigonal warping are indicated for nonarmchair NTs. The same E_{11} and E_{22} transitions occur in the S-SWCNTs, which do not have the inner crossing bands.

I. INTRODUCTION

Correlated electron systems often exhibit behavior that are substantively different from what is expected within one-electron (1-e) theory. In particular, the classification of materials as simple metals or semiconductors breaks down for sufficiently strong electron-electron (e-e) interactions. The effects of e-e interactions are particularly strong in low dimension, and carbon-based quasi-one-dimensional (quasi-1D) systems such as π -conjugated polymers, semiconducting and conducting charge-transfer solids, and carbon nanotubes commonly exhibit novel behavior ascribed to e-e interactions. Although it is by now generally accepted that Coulomb interactions between the π -electrons are strong in single-walled carbon nanotubes (SWCNTs), they continue to be classified as metallic (M-SWCNTs) and semiconducting (S-SWCNTs), based on the predictions of 1-e theory. Thus, SWCNTs with chirality indices (n,m) are commonly referred to as metallic if $(n-m) = 3j$, where j is an integer including zero, and semiconducting otherwise. Schematic π -electron tight-binding band structures of the armchair ($n=m$) and nonarmchair ($n \neq m$, including $m=0$) M-SWCNTs are shown in Fig. 1. The innermost valence and conduction bands (VB and CB, respectively) have linear dispersions and meet at Dirac points, which constitute the Fermi points here. The crossing innermost bands are missing in the S-SWCNTs; otherwise their bandstructures are similar to that in Fig 1(b). We continue to use the nomenclature based on 1-e theory for simplicity in what follows, with the recognition that simple classifications of SWCNTs may not be entirely meaningful.

In recent years, there has been a strong interest in the consequences of e-e interactions on the photophysics of S-SWCNTs. The bulk of the existing literature is on optical absorptions polarized parallel to the NT axes, where e-e interactions lead to exciton formation. The exciton character of the longitudinally polarized absorptions in S-SWCNTs^{1,2,3,4,5,6,7,8,9,10} is now firmly established. Nonlinear absorption¹¹ and two-photon induced fluorescence^{12,13,14} have demonstrated that the binding energy of the lowest longitudinal optical exciton in S-SWCNTs is substantial relative to the optical gap. Research on optical absorptions polarized *perpendicular* to the NT axes has been less extensive^{7,15,16,17,18}, but the consequences of e-e interactions here are even more dramatic. Within 1-e theory, the perpendicularly polarized absorption occurs exactly at the center of the two lowest longitudinally polarized absorptions (hereafter E_{11} and E_{22} , see Fig. 1). The experimentally observed strong blueshift of the perpendicularly polarized absorption¹⁵ to near E_{22} is due to e-e interactions^{7,16,17,18}.

There exists also a considerable body of theoretical^{19,20,21,22,23,24,25} and experimental^{26,27,28,29} literature on the effects of e-e interactions on the M-SWCNTs, that until recently had focused mostly on transport behavior. Screening of the interactions between the π -electrons in these 1D systems is weak, and the lowest excitations in M-SWCNTs have been shown to correspond to those of a Luttinger liquid (LL) rather than a Fermi liquid. Indeed, it has been claimed¹⁹ that the lowest excitations of an (n,n) armchair M-SWCNTs can be approximately mapped onto those of two-leg “Hubbard ladders”³⁰ with an effective on-site Hubbard repulsion $U_{eff} \sim U/n$, where U is the repulsion between two electrons occupying the same p_z carbon orbital. Given that U is substantial in carbon-based systems^{7,8}, this would suggest that the narrowest armchair nanotubes with diameters $d \simeq 1$ nm are likely Mott-Hubbard semiconductors with both charge- and spin-gaps.^{19,22,23} Although excitations in nonarmchair M-SWCNTs are more complex, it is believed that the low energy physics of these are the same as in the armchair tubes. Finally, while the above discussions concerning the Mott-Hubbard semiconductor nature of the narrowest M-SWCNTs focused on the short-range component of the e-e interactions, the charging energy of a tube is determined primarily by the long-range component, which has also been shown to be weakly screened²⁰. Fitting the experimental charging energy of a M-SWCNT²⁶ with a $1/|x|$ potential, for example, requires a dielectric constant of only 1.4²⁰.

It is in this context that we examine theoretically the photophysics of M-SWCNTs here.

We are concerned not about the lowest excitations involving the electrons occupying the innermost bands in Fig. 1, but optical transitions in the visible region. Electronic transitions leading to optical absorptions within 1-e theory are indicated in Fig. 1. In addition to the VB-to-CB transitions that are polarized parallel to the NT axes, we expect also midgap transitions polarized perpendicular to the NT axes, based on our experience with the S-SWCNTs.^{7,17} Only the absorptions parallel to the NT-axis have been experimentally investigated in M-SWCNTs so far.^{31,32,33,34,35} In view of the weak screening of the e-e interactions in M-SWCNTs (see above), we expect the “large Hubbard U ” description to be appropriate here, *even if these systems are conducting and are not Mott-Hubbard semiconductors*. Note that unlike in true 1D, the Hubbard U has to be larger than a critical value before a metal-to-insulator transition will occur in graphene. Conducting behavior thus is not a signature of reduced U . Taken together with the large atomic U scenario, the 1:1 correspondence of the VB-to-CB transitions in Fig. 1 to those in the S-SWCNTs then suggests that photoexcitations in M-SWCNTs are to excitons with binding energies that are perhaps comparable to those in the S-SWCNTs. This conjecture is, however, in strong contradiction to existing theoretical results.³⁶ Within the latter method the ground state is determined using an *ab initio* approach, which is followed by the determination of the quasiparticle energies within the GW approximation and the solution of the Bethe-Salpeter equation of the two-particle Green’s function. This technique has claimed that binding energies in M-SWCNTs are an order of magnitude smaller than those in S-SWCNTs with comparable diameters. A recent work has also claimed that the experimental E_{22} absorption of the (21,21) armchair M-SWCNT can be fit well within the *ab initio* theory, and that the exciton binding energy in this system is only 0.05 eV³⁵. The absence of two-photon induced fluorescence in M-SWCNTs (because of the inner VB and CB) has prevented the direct measurement of exciton binding energies. It then becomes imperative to investigate the photophysics of M-SWCNTs theoretically using other approaches.

In the present paper, we report the results of many-body calculations of the photophysics of M-SWCNTs, based on a molecular Hamiltonian that has previously yielded quantitatively accurate results for the absolute exciton energies, exciton binding energies and nonlinear absorption in S-SWCNTs^{7,8,11,17}. The exciton binding energies we obtain for M-SWCNTs are considerably larger than those found in reference 36. In agreement with the earlier LL theories, our results indicate that screening of the electron-hole interactions in M-SWCNTs

is considerably weaker than in conventional metals.

In section II we present our π -electron Hamiltonian and indicate how the parameters of the Hamiltonian are obtained. We then give a brief justification of the choice of our parameters. In section III.A we present our theoretical results for linear and nonlinear absorptions in the M-SWCNTs. Our results for the absolute exciton energies are in excellent agreement with experiments for all twelve M-SWCNTs that we have studied. Our calculated exciton binding energies are much larger than those predicted within the *ab initio* theory. In section III.B we compare our calculated absorption spectrum of the (21,21) M-SWCNT with the experimental spectrum.³⁵ Again, excellent agreement between the theoretical and experimental absorption spectra is obtained. Finally, in section III.C we present our predicted theoretical absorption spectra polarized perpendicular to the NT axes. As with the S-SWCNTs,^{7,16,17,18} the perpendicularly polarized absorptions show dramatic effects of e-e interactions. Unlike in the S-SWCNTs, though, the lowest perpendicularly polarized absorptions will occur *below* the lowest longitudinal absorption in the M-SWCNTs. In section IV we present our conclusions, focusing on the difference between our results and those obtained within the *ab initio* approach.³⁶

II. π -ELECTRON MODEL AND ITS PARAMETRIZATION

We investigate theoretically the photophysics of M-SWCNTs within the same π -electron Pariser-Parr-Pople (PPP)³⁷ model that we have used for the S-SWCNTs^{7,8} and planar π -conjugated polymers³⁸,

$$H = -t \sum_{\langle ij \rangle, \sigma} (c_{i,\sigma}^\dagger c_{j,\sigma} + H.C.) + U \sum_i n_{i,\uparrow} n_{i,\downarrow} + \sum_{i < j} V_{ij} (n_i - 1)(n_j - 1) \quad (1)$$

where $c_{i,\sigma}^\dagger$ creates a π -electron of spin σ on carbon atom i , $n_{i,\sigma} = c_{i,\sigma}^\dagger c_{i,\sigma}$ is the number of electrons on atom i with spin σ and $n_i = \sum_\sigma n_{i,\sigma}$ is the total number of electrons on atom i . Here t is the nearest neighbor one-electron hopping, U and V_{ij} are the on-site and intersite Coulomb interactions. We parametrize V_{ij} as^{7,8,38}

$$V_{ij} = \frac{U}{\kappa \sqrt{1 + 0.6117 R_{ij}^2}} \quad (2)$$

where R_{ij} is the distance between carbon atoms i and j in Å, and κ is the background dielectric constant. Since full many-body calculations are not possible within Eq. 1, we use the single-configuration interaction (SCI), which retains all matrix elements between single-excitations from the Hartree-Fock (HF) ground state. Calculations reported below are for 60 or more unit cells, with open boundary conditions^{7,8}.

The three independent parameters within Eq. 1 are t , U and κ . The nearest neighbor hopping integral is widely accepted to be 2.4 eV in planar π -conjugated systems.³⁸ The hopping in SWCNTs is smaller because of the curvature, which decreases the overlaps between neighboring p_z orbitals. A smaller t of 2.0 eV for S-SWCNTs was determined from careful fitting of the experimental data.⁸ Since the curvature effects in M-SWCNTs are the same as in S-SWCNTs, we use the same $t = 2.0$ eV as in the S-SWCNTs. Not surprisingly, the Hubbard on-site repulsion U is found to be the same in both π -conjugated polymers³⁸ and S-SWCNTs^{7,8,17}, viz., 8 eV, which would place both these classes of materials among strongly correlated-electron systems. In the context of a different class of 1D correlated-electron materials, organic charge-transfer solids, it has been shown by numerous authors in the past that the short-range e-e interaction, in particular the Hubbard U , remains practically unchanged between the $\frac{1}{2}$ -filled band semiconductors and the non- $\frac{1}{2}$ -filled conductors^{39,40,41,42,43}. This conclusion has been substantiated by more recent work^{44,45} and is also in agreement with theories of high temperature superconductors, within which the undoped Mott-Hubbard semiconductors and the doped conductors and superconductors are generally assumed to have the same U . Based on prior work, we therefore expect the Hubbard U to be the same in M-SWCNTs and S-SWCNTs, and use $U = 8$ eV in our calculations reported here.

The long range interaction V_{ij} in M-SWCNTs, however, can be different from S-SWCNTs due to screening, and this is taken into account by modifying κ . We arrive at the appropriate κ by comparing the experimental lowest longitudinal exciton energies in three different M-SWCNTs: (8,8) armchair, (12,0) zigzag and (9,6) chiral with PPP-SCI energies, calculated using multiple values of κ . In Table I we show our comparisons of the calculated and experimental quantities for the (8,8), (12,0) and (9,6) M-SWCNTs. The two nonarmchair M-SWCNTs, in which E_{11} splits into a lower E_{11}^- and an upper E_{11}^+ due to trigonal warping³¹, provide rigorous tests of our theory. As seen in the Table, while the κ appropriate for M-SWCNTs is certainly larger than the value 2 used for S-SWCNTs,⁸ $\kappa > 3$ yields exciton

energies that are too small. The only exception to this is E_{11}^- for the (12,0) NT. Note, however, that (i) this is the narrowest NT considered (as has been emphasized in reference 8, π -electron theory becomes less quantitative for small d), and (ii) even here the best fit to E_{11}^+ is with $\kappa = 3$. We have therefore chosen $\kappa = 3$ in what follows.

Justification of the choice of our Hamiltonian and our parameters come from two considerations. First, previous theoretical works on M-SWCNTs have already emphasized weak screening of e-e interactions in M-SWCNTs.^{19,20,21,22,23,24,25} Our determination that κ in M-SWCNTs is only slightly larger than that in S-SWCNTs agrees with the conclusion of reference 20 that fitting the charging energy in M-SWCNTs requires a relatively small dielectric constant. Second, in the case of S-SWCNTs, the PPP-SCI approach has provided the best agreement with experimental absolute exciton energies and exciton binding energies to date for nanotubes with $d \geq 1$ nm. The *maximum* difference between our previously calculated and experimental E_{11} for S-SWCNTs with diameters in this range is 0.05 eV, while for slightly narrower tubes with d between 0.75 - 1.0 nm, this difference is 0.1 eV⁸. Our calculated exciton binding energies of 0.4 to 0.3 eV for S-SWCNTs with $d \sim 0.8 - 1.0$ nm are within 0.04 eV of the experimental quantities on the average⁸. Our calculated energies of absorptions polarized perpendicular to the NT axes for four different S-SWCNTs with $d \sim 1$ nm are also within 0.1 eV of experimental values.¹⁷

III. RESULTS

A. Linear and nonlinear absorptions in M-SWCNTs

In Table II we present our calculated and experimental^{31,32,33,34} absolute energies of the excitons for twelve different M-SWCNT's with $d > 0.8$ nm. We compare theoretical results mostly against the experimental results of reference 31, which is the only work that reports both E_{11}^- and E_{11}^+ for the nonarmchair M-SWCNTs. We obtain excellent fits to experiments in all cases. Importantly, our calculations reproduce almost quantitatively the small energy differences between E_{11}^- and E_{11}^+ . Our largest deviations, 0.18 eV for E_{11}^- and 0.12 eV for E_{11}^+ , are for the (10,1) NT with smallest d . Theoretical and experimental results agree particularly well for the (15,0) and the (13,1) NTs, for which the experimental quantities reported in the different references are close.

TABLE I: Calculated and experimental³¹ exciton energies for three M-SWCNTs with $t = 2.0$ eV and $U = 8$ eV, and several different κ .

(n,m)	d (nm)	κ	E_{11}^- (eV)		E_{11}^+ (eV)	
			PPP	Expt.	PPP	Expt.
(8,8)	1.10	2.0	2.35	2.11	—	—
		2.2	2.26		—	
		3.0	2.07		—	
		3.5	2.00		—	
		4.0	1.94		—	
(12,0)	0.95	2.0	2.57	2.16	2.71	2.47
		2.2	2.48		2.63	
		3.0	2.28		2.49	
		3.5	2.21		2.42	
		4.0	2.15		2.37	
(9,6)	1.04	2.0	2.35	2.15	2.52	2.22
		2.2	2.30		2.45	
		3.0	2.14		2.25	
		3.5	2.08		2.17	
		4.0	2.03		2.12	

TABLE II: Calculated and experimental exciton energies in M-SWCNTs, and the calculated binding energies of the excitons

(n,m)	d (nm)	E_{11}^- (eV)		E_{11}^+ (eV)		E_{b1} (eV)
		PPP	Expt.	PPP	Expt. ^a	PPP
(7,7)	0.96	2.31	2.34 ^a , 2.43 ^b	—	—	0.31
(8,8)	1.10	2.07	2.11 ^a , 2.22 ^b	—	—	0.28
(9,9)	1.24	1.88	1.91 ^a , 2.03 ^b , 2.02 ^c	—	—	0.25
(10,10)	1.38	1.72	1.75 ^a , 1.89 ^{b,c}	—	—	0.23
(10,1)	0.84	2.51	2.33 ^a , 2.28 ^b , 2.38 ^c	2.83	2.71	0.30
(9,3)	0.86	2.47	2.36 ^a , 2.35 ^b , 2.43 ^c	2.71	2.61	0.29
(8,5)	0.90	2.42	2.37 ^a , 2.47 ^{b,c}	2.54	2.47	0.29
(12,0)	0.95	2.28	2.16 ^{a,b}	2.49	2.47	0.27
(10,4)	0.99	2.22	2.17 ^a , 2.22 ^b	2.37	2.33	0.27
(9,6)	1.04	2.14	2.15 ^a , 2.23 ^b , 2.24 ^c	2.25	2.22	0.27
(13,1)	1.07	2.07	2.01 ^a , 2.02 ^b , 2.06 ^c	2.26	2.24	0.25
(15,0)	1.19	1.91	1.86 ^{a,c} , 1.88 ^b	2.03	2.06	0.24

^aFrom Ref. 31. ^bFrom Refs. 33 and 34. ^cFrom Ref. 32.

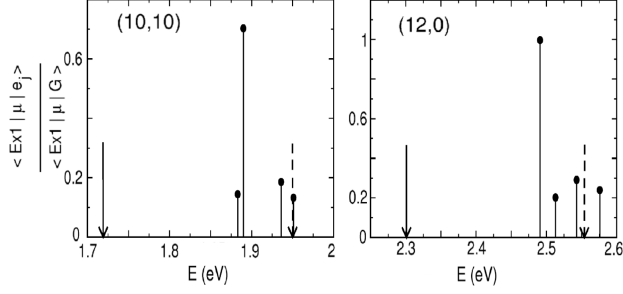


FIG. 2: Transition dipole couplings between above-gap excited states j and the optical exciton Ex1, relative to the dipole coupling between Ex1 and the ground state G, in the (10,10) and (12,0) M-SWCNTs. The solid and dashed arrows denote the energy locations of the optical exciton and the threshold of the continuum band, respectively.

Table II also lists our calculated binding energies E_{b1} , which we define as the energy difference between the lower threshold of the continuum band and the E_{11} (E_{11}^-) exciton in armchair (nonarmchair) M-SWCNTs. Within the SCI approximation, the Hartree-Fock threshold gives the threshold of the continuum.^{7,8,38} The E_{b1} in all cases are significantly larger than those obtained within *ab initio* theory³⁶, and are 70-80% of the exciton binding energies in S-SWCNTs with similar diameters.⁸ For M-SWCNTs with $d \sim 1$ nm, for instance, the *ab initio* work had predicted $E_{b1} \sim 0.05$ eV, while the PPP values are 0.25 - 0.30 eV. Our ability to reproduce the small energy differences between E_{11}^- and E_{11}^+ gives us confidence about our calculated E_{b1} .

The predicted large E_{b1} can be verified from pump-probe measurements of excited state absorptions¹¹. In Figs. 2(a) and (b) we show the calculated normalized transition dipole couplings between the lowest optical exciton and higher energy two-photon states in the (10,10) and (12,0) M-SWCNTs. As in the S-SWCNTs¹¹, there occurs a dominant two-photon exciton that is strongly dipole-coupled to the optical exciton, and that therefore should be visible as excited state absorption. We find similar results in the other metallic NTs. The energy difference between the two-photon exciton and the optical exciton is the lower bound to E_{b1} .

B. Optical absorption in the (21,21) M-SWCNT

The absorption spectrum in the E_{22} region of the (21,21) M-SWCNT ($d = 2.9$ nm) has recently been obtained experimentally.³⁵ The absorption band is asymmetric, with weak but

significant absorption on the high energy side of the peak in the absorption (see Fig. 3). Based on comparisons with the rigidly downshifted symmetric E_{44} absorption spectrum of the (16,15) S-SWCNT and lineshape analysis, the authors of this work concluded that E_{b2} in (21,21) M-SWCNT is only 0.05 eV. As *ab initio* calculation for the wide (21,21) M-SWCNT is difficult, the authors used the calculated *ab initio* E_{11} transition of the (10,10) S-SWCNT ($d = 1.38$ nm) to fit the experimental E_{22} absorption of the (21,21) M-SWCNT, since within band theory the two one-electron gaps have the same origin and are the same in magnitude (the absorptions to the exciton and the continuum band were, however, calculated separately and superimposed in this work). The *ab initio* E_{b1} of the (10,10) M-SWCNT is also ~ 0.05 eV, seemingly supporting the conjecture that the E_{11} exciton of the (10,10) M-SWCNT and the E_{22} exciton of the (21,21) M-SWCNT are equivalent even when e-e interactions are significant. Note that our calculated E_{b1} in the (10,10) M-SWCNT in Table II is, however, significantly larger (0.23 eV), implying that substituting the E_{11} spectrum of the (10,10) NT for the E_{22} spectrum of the (21,21) NT may not be appropriate.

We have calculated directly the entire absorption spectrum in the E_{22} region of the (21,21) M-SWCNT within a single calculation using the PPP-SCI approach. Comparison of the theoretical and experimental absorption spectra provides a direct test of our theory. Our calculated E_{22} is 1.75 eV, in good agreement with the experimental E_{22} of 1.87 eV.³⁵ The calculated exciton energy is indeed close to E_{11} in the (10,10) M-SWCNT (see Table II). In Fig. 3 we compare our calculated absorption spectrum, rigidly shifted by the 0.12 eV energy difference between our calculated and the experimental E_{22} , with the experimental data points of reference 35. Apart from this rigid shift, the fitting is excellent: the calculated spectrum reproduces both the asymmetric line shape as well as the high energy tail. The latter is not due to absorption to the continuum band³⁶, but is due to weak absorptions to higher excitons that lie below the continuum band threshold. Similar absorptions to higher excitons are known to contribute to the asymmetric lineshapes of absorptions within the PPP Hamiltonian, whenever the exciton binding energy is relatively small³⁸, and occur also in the perpendicularly-polarized absorptions in S-SWCNTs with $d \sim 1$ nm, where the transverse excitons have binding energies of 0.1 - 0.15 eV (see the experimental absorption spectra in Fig. 3(d) in reference 15 and the calculated absorption spectra in Fig. 3 of reference 17). For comparison to the absorption to an exciton in a S-SWCNT, as was done in reference 35, we have superimposed in Fig. 3 the calculated absorption band in the E_{22}

region of the (19,0) S-SWCNT, again rigidly shifted such that the peaks of the two calculated absorptions match. According to the prescription of reference 35, the threshold of the E_{22} continuum of the (21,21) M-SWCNT should occur at the energy where the absorptions of the semiconducting and the metallic NTs begin to diverge, viz., at ~ 1.92 eV from Fig. 1(c). The actual calculated threshold of the continuum, indicated by the arrow in Fig. 3, is, however, at a significantly higher energy. We calculate E_{b2} in the (21,21) M-SWCNT to be 0.12 eV, nearly half that of the (10,10) M-SWCNT.

For S-SWCNTs, E_{b1} and E_{b2} for the same system are comparable. Furthermore, exciton binding energies in S-SWCNTs decrease with diameter.^{7,8} If one assumes both of these to be true in M-SWCNTs, comparable E_{b2} in the (21,21) M-SWCNT and E_{b1} in the (10,10) M-SWCNT, as calculated within the *ab initio* theory are not expected. The large difference between our calculated E_{b1} of 0.23 eV in the (10,10) M-SWCNT (see Table II) and E_{b2} of 0.12 eV in the (21,21) M-SWCNT, *in spite of the same absolute energies of the corresponding excitons*, in contrast, is in agreement with the diameter dependence in the semiconductors. The difference in the two binding energies is not surprising. The thresholds of the continua in our calculations correspond to the Hartree-Fock thresholds within Eq. 1. These energies are different for the (10,10) and (21,21) M-SWCNTs. even as their tight-binding thresholds are nearly the same. Although the lowest excitations in the M-SWCNTs do not necessarily reflect the behavior of the higher energy excitations, it is interesting that the mapping suggested in reference 19 predicts a U_{eff} in the (21,21) M-SWCNT that is half the U_{eff} in the (10,10) M-SWCNT.

C. Perpendicularly polarized absorption in M-SWCNTs

We now make a verifiable prediction concerning optical absorption polarized perpendicular to the NT axes. The strong blueshift of the transverse absorption from the exact center of E_{11} and E_{22} in the S-SWCNTs¹⁵ is due to e-e interactions^{7,16,17,18}. Degenerate basis functions reached by E_{12} and E_{21} excitations here from new correlated electron eigenstates that are odd and even superpositions of these basis functions. The redshifted odd superposition is optically forbidden, while the blueshifted even superposition is optically allowed.^{7,17} We anticipate the degenerate perpendicularly-polarized one-electron transitions in M-SWCNTs (see Fig. 1) to be also similarly split by e-e interactions, giving rise to a redshifted forbidden

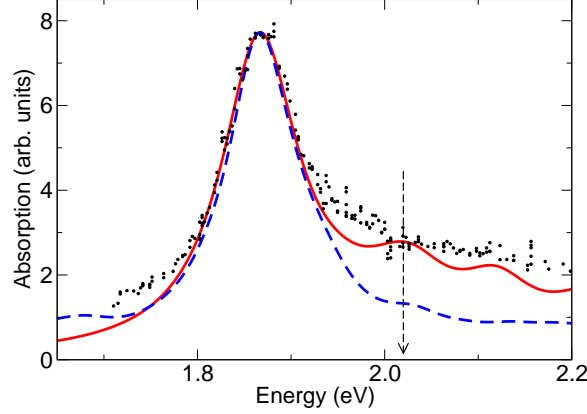


FIG. 3: (Color online) Calculated absorption spectrum (red curve) in the E_{22} region of the (21,21) M-SWCNT, superimposed on the experimental data³⁵ (black dots). The calculated spectrum has been shifted rigidly by 0.12 eV. The arrow gives the calculated threshold of the continuum band. The blue dashed curve is the calculated E_{22} absorption of the (19,0) S-SWCNT, shifted rigidly so that the peaks of the two calculated spectra match. Linewidths of 0.05 eV and 0.04 eV, respectively, for the (21,21) and (19,0) NT's, have been used.

transition and a blueshifted allowed absorption. The novel feature here, however, is that the lowest perpendicularly polarized absorption is “subgap”, occurring below the lowest longitudinal optical absorption.

In Figs. 4(a) and (b) we have shown our calculated perpendicularly polarized absorptions for the (7,7) and the (12,0) M-SWCNTs, where we have also included the longitudinal E_{11} absorptions. The subgap perpendicularly polarized absorptions are blueshifted substantially from the exact midgap. In spite of this strong Coulomb effect, we find the binding energy of the perpendicular absorption in the M-SWCNTs to be nearly zero.

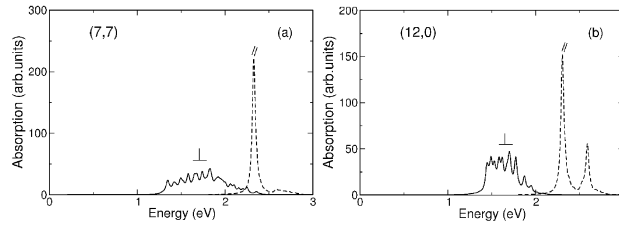


FIG. 4: Calculated optical absorptions polarized perpendicular to the NT axes in the (a) (7,7) and (b) (12,0) M-SWCNTs. The E_{11} absorptions are included for comparison (the splitting of E_{11} in (b) is due to trigonal warping). The zero frequency Drude absorptions are not shown.

IV. CONCLUSIONS

To conclude, M-SWCNTs are expected to exhibit optical behavior very similar to S-SWCNTs, with only slightly smaller exciton binding energies. We emphasize that within the PPP Hamiltonian of Eq. 1, determining the absolute energy of the exciton and its binding energy are *not* different problems. In the limit of large U with only nearest neighbor intersite e-e interaction V_1 , for example, the exciton in a purely 1D system occurs at energy $U - V_1$ while the conduction band is centered at U ⁴⁶. *Thus, in this limit, once the U is fixed, it is not possible to obtain the precise exciton energy but incorrect exciton binding energy.* For moderate U , where the hopping term plays a stronger role, it is necessary to also fix the t ; but once again, for fixed U and t , correct determination of the absolute exciton energy within Eq. 1 necessarily implies that the continuum band threshold has also been correctly evaluated. Based on our argument in section I that the atomic U is the same in the S-SWCNTs and the M-SWCNTs then, the excellent fits to the absolute exciton energies in Table II, as well as to the optical absorption spectrum in Fig. 3, imply that our estimates of the exciton binding energies are correct. The large E_b implies weak screening of Coulomb interactions. As we have pointed out, weak screening of e-e interactions in these 1D materials^{19,20,21,22,23,24,25} suggests that simple concepts of metallic screening do not apply.

The discrepancy between the predictions of the molecular model used here and the *ab initio* approach is not unexpected. Note that even for the S-SWCNTs, the calculated exciton binding energies within the two methods are widely different, with the *ab initio* approach predicting binding energies⁴ that are often twice the experimental values.¹³ Although it has been suggested that the experimental binding energies reflect screening of e-e interactions due to intertube interactions, and the true single tube binding energies are much larger and close to the *ab initio* predictions, an alternate possibility is that the molecular model, which reproduces experimental longitudinal *and* transverse exciton energies and exciton binding energies quantitatively, is simply better calibrated to handle systems with large Hubbard interaction. The difficulty of treating strong on-site e-e interaction within density functional based theories, for instance, is well known.^{47,48,49}

SWCNTs are currently of strong interest because of their potential technological applications. Our demonstration that M-SWCNTs will exhibit photophysics similar to the semiconductors, even as their transport behavior correspond to that of unconventional

conductors, may introduce new and exciting possibilities.

V. ACKNOWLEDGMENTS

We are grateful to Professors F. Wang and T. F. Heinz for sending us the experimental absorption data for the (21,21) NT, and to Professors A. Shukla and Z. V. Vardeny for critical reading of the manuscript. This work was supported by NSF grant number DMR-0705163.

-
- ¹ T. Ando, J. Phys. Soc. Jpn. **66**, 1066 (1997).
 - ² M. F. Lin, Phys. Rev. B **62**, 13153 (2000).
 - ³ C. L. Kane and E. J. Mele, Phys. Rev. Lett. **90**, 207401 (2003).
 - ⁴ C. D. Spataru, S. Ismail-Beigi, L. X. Benedict, and S. G. Louie, Phys. Rev. Lett. **92**, 077402 (2004).
 - ⁵ E. Chang, G. Bussi, A. Ruini, and E. Molinari, Phys. Rev. Lett. **92**, 196401 (2004).
 - ⁶ V. Perebeinos, J. Tersoff, and Ph. Avouris, Phys. Rev. Lett. **92**, 257402 (2004).
 - ⁷ H. Zhao and S. Mazumdar, Phys. Rev. Lett. **93**, 157402 (2004).
 - ⁸ Z. Wang, H. Zhao, and S. Mazumdar, Phys. Rev. B **74**, 195406 (2006).
 - ⁹ M. S. Dresselhaus, G. Dresselhaus, R. Saito, and A. Jorio, Annu. Rev. Phys. Chem. **58**, 719 (2007).
 - ¹⁰ G. D. Scholes, S. Tretiak, T. J. McDonald, W. K. Metzger, C. Engtrakul, G. Rumbles and M. J. Heben, J. Phys. Chem. C, **111**, 11139 (2007).
 - ¹¹ H. Zhao, S. Mazumdar, C.-X. Sheng, M. Tong, and Z. V. Vardeny, Phys. Rev. B **73**, 075403 (2006).
 - ¹² F. Wang, G. Dukovic, L. E. Brus, and T. F. Heinz, Science **308**, 838 (2005).
 - ¹³ G. Dukovic, F. Wang, D. Song, M. Y. Sfeir, T. F. Heinz and L. E. Brus, Nano Lett. **5**, 2314 (2005).
 - ¹⁴ J. Maultzsch *et al.*, Phys. Rev. B **72**, 241402(R) (2005).
 - ¹⁵ Y. Miyauchi, M. Oba, and S. Maruyama, Phys. Rev. B **74**, 205440 (2006).
 - ¹⁶ S. Uryu and T. Ando, Phys. Rev. B **74**, 155411 (2006).
 - ¹⁷ Z. Wang, H. Zhao, and S. Mazumdar, Phys. Rev. B **76**, 115431 (2007).

- ¹⁸ S. Kilina, S. Tretiak, S. K. Doorn, Z. Luo, F. Papadimitrakopoulos, A. Piryatinski, A. Saxena, and A. R. Bishop, Proc. Natl. Acad. Sci. **105**, 6797 (2008).
- ¹⁹ L. Balents and M. P. A. Fisher, Phys. Rev. B **55**, R11973 (1997).
- ²⁰ R. Egger and A. O. Gogolin, Phys. Rev. Lett. **79**, 5082 (1997).
- ²¹ C. Kane, L. Balents and M. P. A. Fisher, Phys. Rev. Lett. **79**, 5086 (1997).
- ²² Y. A. Krotov, D. H. Lee and S. G. Louie, Phys. Rev. Lett. **78**, 4245 (1997).
- ²³ H. Yoshioka and A. A. Odintsov, Phys. Rev. Lett. **82**, 374 (1999).
- ²⁴ A. A. Odintsov and H. Yoshioka Phys. Rev. B **59**, R10457 (1999).
- ²⁵ J. E. Bunder and H.-H. Lin, Phys. Rev. B **75**, 075418 (2007).
- ²⁶ S. J. Tans, M. H. Devoret, H. Dai, A. Thess, R. E. Smalley, L. J. Geerligs, and C. Dekker, Nature **386**, 474 (1997).
- ²⁷ S. J. Tans, M. H. Devoret, R. J. O. Groeneveld, and C. Dekker, Nature **394**, 761 (1998).
- ²⁸ M. Bockrath, D. H. Cobden, P. L. McEuen, N. G. Chopra, A. Zettl, A. Thess, R. E. Smalley, Science **275**, 1922 (1997).
- ²⁹ M. Bockrath, D. H. Cobden, A. G. Rinzler, R. E. Smalley, L. Balents and P. L. McEuen, Nature **397**, 598 (1999).
- ³⁰ E. Dagotto and T. M. Rice, Science **271**, 618 (1996).
- ³¹ M. S. Strano *et al.*, Nano Lett. **3**, 1091 (2003).
- ³² H. Telg, J. Maultzsch, S. Reich, F. Hennrich, and C. Thomsen, Phys. Rev. Lett. **93**, 177401 (2004).
- ³³ C. Fantini, A. Jorio, M. Souza, M. S. Strano, M. S. Dresselhaus and M. A. Pimenta, Phys. Rev. Lett. **93**, 147406 (2004).
- ³⁴ C. Fantini, A. Jorio, A. P. Santos, V. S. T. Peressinotto, and M. A. Pimenta, Chem. Phys. Lett. **439**, 138 (2007).
- ³⁵ F. Wang *et al.*, Phys. Rev. Lett. **99**, 227401 (2007).
- ³⁶ J. Deslippe, C. D. Spataru, D. Prendergast, and S. G. Louie, Nano Lett. **7**, 1626 (2007)
- ³⁷ R. Pariser, and R. G. Parr, J. Chem. Phys. **21**, 466 (1953). J. A. Pople, Trans. Faraday Soc. **49**, 1375 (1953).
- ³⁸ M. Chandross and S. Mazumdar, Phys. Rev. B **55**, 1497 (1997).
- ³⁹ Z. G. Soos, Ann. Rev. Phys. Chem. **25**, 121 (1974).
- ⁴⁰ J. B. Torrance, Acc. Chem. Res. **12**, 79 (1979).

- ⁴¹ J. Hubbard, Phys. Rev. B **17**, 494 (1978).
- ⁴² S. Mazumdar and A. N. Bloch, Phys. Rev. Lett. **50**, 207 (1983).
- ⁴³ S. Mazumdar and S.N. Dixit, Phys. Rev. B **34**, 3683 (1986).
- ⁴⁴ R. Claessen, M. Sing, U. Schwingenschlogl, P. Blaha, M. Dressel and C. S. Jacobsen, Phys. Rev. Lett. **88**, 096402 (2002).
- ⁴⁵ D. Bozi, J. M. P. Carmelo, K. Penc and P. D. Sacramento, J. Phys. Cond. Matter, **20**, 022205 (2008).
- ⁴⁶ D. Guo, S. Mazumdar, S.N. Dixit, F. Kajzar, F. Jarka, Y. Kawabe and N. Peyghambarian, Phys. Rev B **48**, 1433 (1993).
- ⁴⁷ G. Kotliar, S. Y. Savrasov, K. Haule, V. S. Oudovenko, P. Parcollet and C. A. Marianetti, Rev. Mod. Phys. **78**, 865 (2006).
- ⁴⁸ S. Y. Savrasov, G. Kotliar and E. Abrahams, Nature **410**, 793 (2001).
- ⁴⁹ A. J. Cohen, P. Mori-Sánchez and W. Yang, Science **321**, 792 (2008).